Analysis of GRIN Lenses with PEC Elements Using a 2D Cylindrical Electromagnetic Solver

Vincent Kaschten*†, Dimitri Lederer*, Christophe Craeye*,
*ICTEAM Institute, UCLouvain, Louvain-la-Neuve, Belgium,
vincent.kaschten@uclouvain.be, dimitri.lederer@uclouvain.be, christophe.craeye@uclouvain.be
†BEA Sensors Europe, Liège, Belgium

***Abstract*—We propose a mathematical formulation for studying the 2D propagation of electromagnetic waves throughout a cylindrical GRIN lens, when the source is located inside the lens. The lens can contain electrically small cylindrical PEC elements, whose effect on the propagation can be analyzed.**

***Index Terms*—GRIN lenses, electromagnetic propagation, cylindrical, PEC.**

I. Introduction

The study of Gradient-Index (GRIN) lenses, and particularly of electromagnetic propagation of waves throughout them, has been a subject of interest for a long time [1]. The propagation of a source of electromagnetic radiation located outside such a cylindrical dielectric lens, has been studied both analytically [2] and using full-wave solvers such as CST Microwave Studio [3]. The scattering of a wave by a cylindrical body made of an electrically large metallic core (PEC) surrounded by dielectric layers has also been studied, with a source located inside [4][5] or outside [6][7][8] the cylindrical body. Recently, the scattering by a dielectric cylindrical body surrounded by metallic elements wrapped around it has also been studied [9][10], problem already addressed earlier in 2D [11] by use of the semi-analytic Method of Regularization. In this paper, we develop a 2D full-wave solver in cylindrical geometry, assuming infinite length along $\hat{z}$ for all elements. Our solver is based on previous work [2], which we extend to a case where the lossy body is made of concentric cylindrical shells, mimicking a discretized GRIN lens, where the source is located inside the cylinder, as well as a case where the lossy body features a number of electrically small PEC shorting pins. The paper is organized as follows: Section II sets the problem for a homogeneous dielectric lens, Section III extends it to a GRIN lens, Section IV introduces the PEC elements in the lens and Section V provides a conclusion.

II. Homogeneous Lenses

Let us consider a cylindrical coordinate system $(\hat{\rho}, \hat{\phi}, \hat{z})$ in which we represent an incident wave by an infinite linear source located in a medium of relative dielectric permittivity ϵ_r at $(\rho, \phi) = (\rho', 0)$ and oriented along $\hat{z}$, see Fig. 1. For the sake of simplicity, we consider the wave with $k_z = 0$ (the current does not vary along $\hat{z}$) and vertically polarized, such that E_ϕ and H_z components are equal to zero. The analysis of such fields from line sources next to such lenses has been studied in several papers already [2]. The incident field $E_z^i(\rho, \phi, z)$ is expressed as a sum of centred cylindrical harmonics

$$E_z^i = \begin{cases} \displaystyle\sum_{m=-\infty}^{+\infty} e^{jm\phi} C_m J_m(k_\rho \rho) \text{ for } \rho \leq \rho' \\ \displaystyle\sum_{m=-\infty}^{+\infty} e^{jm\phi} C'_m H_m^{(2)}(k_\rho \rho) \text{ for } \rho \geq \rho', \end{cases} \tag{1}$$

and the H-field components are directly obtained using

$$H_\phi^i = \left(\frac{-j\omega\epsilon_r\epsilon_0}{k_\rho^2} \right) \frac{\partial E_z}{\partial \rho}. \tag{2}$$

The decomposition into centred cylindrical harmonics is interesting because boundary conditions can be applied to each harmonic individually. The coefficients of the incident fields (for the m^{th} cylindrical harmonic) are computed by applying boundary conditions at the source:

$$C_m = -I_0 \frac{k_\rho^2}{4\omega\epsilon_r\epsilon_0} H_m^{(2)}(k_\rho \rho) \text{ and } C'_m = -I_0 \frac{k_\rho^2}{4\omega\epsilon_r\epsilon_0} J_m(k_\rho \rho). \tag{3}$$

So far, the dielectric lens was not considered. The question is now to determine how the lens will react to the incident field. For that, the reference paper [2] defines the total field $E_z^t(\rho, \phi, z)$ inside the dielectric cylinder of radius a as a sum of centred Bessel functions, and the scattered field $E_z^s(\rho, \phi, z)$ outside as a sum of centred Hankel functions:

$$\begin{cases} E_z^t = \displaystyle\sum_{m=-\infty}^{+\infty} e^{jm\phi} A_m J_m(k_\rho \rho) \text{ for } \rho \leq a \\ E_z^s = \displaystyle\sum_{m=-\infty}^{+\infty} e^{jm\phi} A'_m H_m^{(2)}(k_\rho \rho) \text{ for } \rho \geq a. \end{cases} \tag{4}$$

The scattered field inside the cylinder ($\rho \leq a$) can only consist of Bessel functions, similarly to the incident field in the region $\rho \leq \rho'$. For that reason, and because of the underlying assumption that the source is located outside the cylinder ($\rho' \geq a$), both the incident and scattered field inside the cylinder ($\rho \leq a \leq \rho'$) have the same form and can be combined into the term E_z^t.

For each of the m^{th} harmonic, the incident, scattered and total fields are used to ensure the continuity of the total fields at the cylinder edge. A set of simple 2x2 systems of equations can thus be solved to find the A_m and A'_m coefficients for each harmonic independently.

III. GRIN LENSES

In this paper we analyse lenses in which the dielectric cylinder of radius a is now made of N concentric cylindrical dielectric shells and we propose an extension involving PEC (perfectly electrical conductor) scatterers. The shells are defined by a set of radii $a_n (0 \leq n \leq N)$ such that the n^{th} shell corresponds to $a_{n-1} \leq \rho \leq a_n$, as shown in Fig. 1. The innermost shell includes the origin ($a_0 = 0$) and the outermost shell defines the lens edge, of radius a ($a_N = a$).

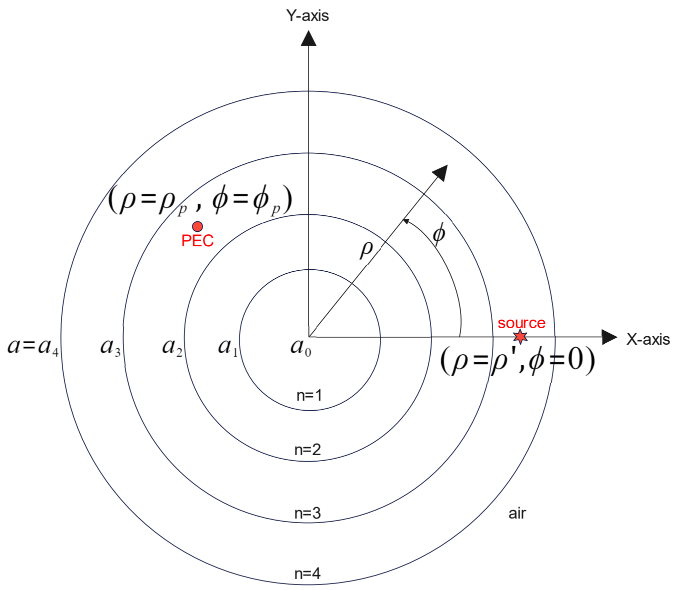

Fig. 1. Geometry of the problem with $N = 4$ shells.

We decide to place the source inside the dielectric cylinder. Following [2] the incident field related to a given source is calculated as before (1)-(3) but taking into account the dielectric permittivity of the shell n' in which the source is placed. The obtained incident field only makes sense in that shell, for that reason we introduce the following notation:

$$E_z^{i,n=n'} = \begin{cases} \sum_{m=-\infty}^{+\infty} e^{jm\phi} C_m J_m(k_\rho \rho) \text{ for } a_{n-1} \leq \rho \leq \rho' \\ \sum_{m=-\infty}^{+\infty} e^{jm\phi} C'_m H_m^{(2)}(k_\rho \rho) \text{ for } a_n \geq \rho \geq \rho' \\ 0 \quad \text{elsewhere,} \end{cases} \tag{5}$$

while noting that $E_z^{i,n\neq n'} = 0$ everywhere.

In practice, one must look for the scattered field in the dielectric regions which might contain sources, and the total field in the dielectric regions which do not contain any. For that reason, we define the scattered field $E_z^{s,n}(\rho, \phi, z)$ inside each shell of index $n \in [1, N]$, and the total field $E_z^t(\rho, \phi, z)$ outside, both expressed as a combination of Hankel functions of the first and second kinds:

$$\begin{cases} E_z^{s,n} = \sum_{m=-\infty}^{+\infty} e^{jm\phi}[A_m^{n,1} H_m^{(1)}(k_\rho \rho) + A_m^{n,2} H_m^{(2)}(k_\rho \rho)] \\ \quad \text{for } \ a_{n-1} \leq \rho \leq a_n \\ E_z^t = \sum_{m=-\infty}^{+\infty} e^{jm\phi} A_m^{2'} H_m^{(2)}(k_\rho \rho) \text{ for } \rho \geq a. \end{cases} \tag{6}$$

Hankel functions of the first kind represent inward propagating waves, whereas those of the second kind represent outward propagating waves. The total field outside can only consist of Hankel functions of the second kind. As before, the continuity of the total fields is ensured at the cylinder edge ($\rho = a$) considering the scattered and incident fields in the outermost shell ($n = N$). The continuity of the total fields must now also be ensured at each interface between two neighbouring dielectric regions:

$$\begin{cases} E_{m,z}^{s,n}(\rho = a_n) + E_{m,z}^{i,n}(\rho = a_n) = \\ E_{m,z}^{s,n+1}(\rho = a_n) + E_{m,z}^{i,n+1}(\rho = a_n) \\ \\ H_{m,z}^{s,n}(\rho = a_n) + H_{m,z}^{i,n}(\rho = a_n) = \\ H_{m,z}^{s,n+1}(\rho = a_n) + H_{m,z}^{i,n+1}(\rho = a_n) \end{cases} \tag{7}$$

for $1 \leq n \leq N - 1$.

For N zones we have a total of $2N + 1$ parameters to determine, while so far $2N$ conditions were written. The last condition is related to the innermost shell, where the superposition of both Hankel functions must correspond to a Bessel function, in other words $A_m^{1,1} = A_m^{1,2}$.

The conditions can be summed up in a system of equations $S_m x_m = b_m$ of size $2N+1$. For the case $N = 2$, the structure of such a system reads as:

$$\begin{bmatrix} 1 & -1 & 0 & 0 & 0 \\ \star & \star & \star & \star & 0 \\ \star & \star & \star & \star & 0 \\ 0 & 0 & \star & \star & \star \\ 0 & 0 & \star & \star & \star \end{bmatrix} \begin{bmatrix} A_m^{1,2} \\ A_m^{1,1} \\ A_m^{2,2} \\ A_m^{2,1} \\ A_m^{2'} \end{bmatrix} = \begin{bmatrix} 0 \\ E_{m,z}^{i,1}(\rho = a_1) - E_{m,z}^{i,2}(\rho = a_1) \\ H_{m,z}^{i,1}(\rho = a_1) - H_{m,z}^{i,2}(\rho = a_1) \\ E_{m,z}^{i,2}(\rho = a_2) \\ H_{m,z}^{i,2}(\rho = a_2) \end{bmatrix} \tag{8}$$

The symbol $\star$ is used for the non-zero elements in the matrix S_m. The vector x_m contains the unknowns A_m while the vector b_m contains incident field values at the different interfaces. In practice, one solves such a system $2M+1$ times, for a finite set of harmonics $m \in [-M, M]$. A single blockdiagonal system $Sx = b$ of size $(2M+1)(2N+1)$ can be written for all harmonics at once, given their independence:

$$\begin{bmatrix} S_{m=-M} & \cdots & 0 \\ \vdots & \ddots & \vdots \\ 0 & \cdots & S_{m=M} \end{bmatrix} \begin{bmatrix} x_{m=-M} \\ \vdots \\ x_{m=M} \end{bmatrix} = \begin{bmatrix} b_{m=-M} \\ \vdots \\ b_{m=M} \end{bmatrix} \tag{9}$$

An illustrative case is shown in Fig. 2 for a GRIN medium of radius $a = 15$mm at 60GHz. The lens is divided into $N = 15$ dielectric zones and implements a Gutman distribution $\epsilon_r(\rho) = 1 + (a/f)^2 - (\rho/f)^2$ with a focal point at $f = 0.75\ a$. The source is placed at $\rho' = f$ and is represented by a red asterisk. As expected, the lens is able to output a plane wave.

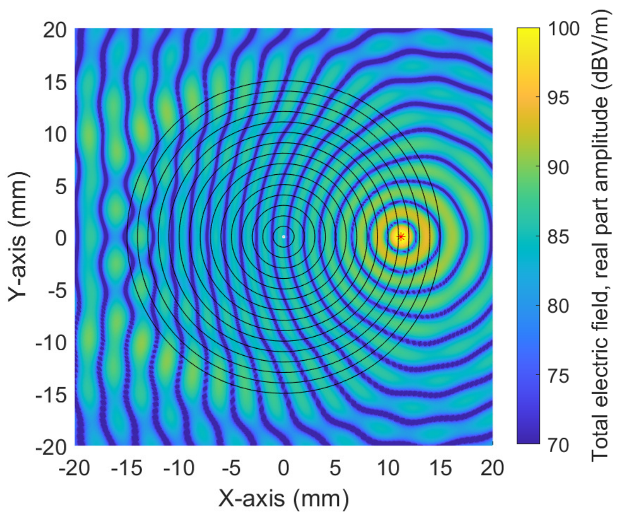

Fig. 2. Source located at the focal point $\rho' = f = 0.75\ a$ of a Gutman lens.

Once the cylindrical harmonic coefficients are obtained for the total field in the region outside the dielectric lens, it is possible to compute the lens radiation pattern. Based on the asymptotic behaviour of Hankel 2 functions in the far region (large $k_\rho \rho$), the total electric field can be rewritten as

$$E_z^t \approx \frac{e^{-jk_\rho \rho}}{\sqrt{k_\rho \rho}} \sqrt{\frac{2}{\pi}} \sum_{m=-M}^{+M} e^{jm(\phi+\pi/2)} e^{j\pi/4} A_m^{2'}, \tag{10}$$

where the radiation pattern $F(\phi)$ clearly appears:

$$F(\phi) = \sqrt{\frac{2}{\pi}}\ e^{j\pi/4} \sum_{m=-M}^{+M} e^{jm(\phi+\pi/2)} A_m^{2'}. \tag{11}$$

The radiation pattern related to Fig. 2 is shown in blue in Fig. 5.

IV. Metallic elements

We add to our solver P cylindrical metallic elements (PEC) placed anywhere inside the lens, at positions (ρ_p, ϕ_p) for $p \in [1, P]$ as shown in Fig. 1, of radius a_p and oriented the same way as the dielectric cylinder (axis along $\hat{z}$). We model those PEC elements by an additional incident field $E_{z,p}^{i,n}$ centred on the PEC, computed as before (1)-(3) for a source intensity $I_0 = 1$ and considering the dielectric permittivity of the dielectric shell n_p in which the PEC is located. We rely for that on Pocklington's approximation, which states the equivalence of generated fields between a current source located on the PEC centre, and a current source distributed over the PEC perimeter. An underlying condition is that the PEC radius a_p be very small compared to the wavelength.

The intensities of each element (relative to the source I_0) are represented by I_p. The m^{th} cylindrical harmonic of the incident field is now the sum

$$E_{m,z}^{i,n} = E_{m,z,source}^{i,n} + \sum_{p=1}^{P} I_p e^{-jm\phi_p} E_{m,z,p}^{i,n} \tag{12}$$

In the systems of equations $S_m x_m = b_m$ expressed in Section III, the vectors b_m contain values of incident fields at the interfaces. Those systems of equations can be rewritten adding the contributions of the PEC elements:

$$S_m x_m = b_m \Leftrightarrow S_m x_m - \sum_{p=1}^{P} I_p b_{m,p} = b_{m,source} \tag{13}$$

The quantities I_p are now additional unknowns of our model. We need to express P additional conditions. A PEC must satisfy the condition that there can be no electric field tangent to its surface. Given our representation of PEC as metallic cylinders oriented along $\hat{z}$ and the electric field having only components along $\hat{z}$, the condition simply states that $E_z^t(\rho_p, \phi_p) = 0$ for $p \in [1, P]$. That condition cannot be solved for each harmonic separately, therefore it is required to solve a single system of equations (9) for all harmonics.

The total electric field is the sum of many contributions:

- the incident field from the source,
- the incident field from each PEC, including the one under observation,
- the scattered field from the lens.

The total electric field observed at the PEC element q located in dielectric shell n_q is thus given by

$$\sum_{m=-M}^{+M} \left(E_{m,z,source}^{i,n_q} + \sum_{p=1}^{P} I_p e^{-jm\phi_p} E_{m,z,p}^{i,n_q} + E_{m,z}^{s,n_q} \right) e^{jm\phi_q}. \tag{14}$$

The incident field from the source is entirely known, such that we can define

$$K_0(q) = \sum_{m=-M}^{+M} E_{m,z,source}^{i,n_q}(k_\rho \rho_q)\ e^{jm\phi_q}. \tag{15}$$

The contribution of the PEC $p \in [1, P]$ on the PEC element $q \in [1, P]$ depends on the unknowns I_p. We define

$$K_1(q,p) = \sum_{m=-M}^{+M} E^{i,n_q}_{m,z,p}(k_\rho \rho_q)\ e^{jm(\phi_q - \phi_p)} \tag{16}$$

such that the contribution can be written

$$\sum_{p=1}^{P} I_p\ K_1(q,p). \tag{17}$$

Let us remind that $E^{i,n_q}_{m,z,p} = 0$ unless $n_q = n_p$. For the diagonal elements of K_1, corresponding to the incident field from the PEC element p on itself, the contribution is not calculated on the PEC center (where the electric field diverges) but rather at the distance a_p from its center, according to Pocklington's approximation. For that, we use the expression of the incident field based on $H^{(2)}_0(k_\rho \rho)$ and evaluate it for $\rho = a_p$. For all other contributions above and below, the evaluation of the field is done on the PEC centre.

The effect of the scattered field from the lens depends on the unknowns inside the vectors x_m, based on the dielectric shell n_q in which the PEC is located. We define

$$K^1_m(q,m) = H^{(1)}_m(k_\rho \rho_q) \text{ and } K^2_m(q,m) = H^{(2)}_m(k_\rho \rho_q) \tag{18}$$

such that the contribution can be written

$$\sum_{m=-M}^{+M} \left(A^{n_q,1}_m K^1_m(q,m) + A^{n_q,2}_m K^2_m(q,m)\right). \tag{19}$$

The PEC conditions can eventually be rewritten for each element $q \in [1, P]$ as

$$-\sum_{m=-M}^{+M} \left(A^{n_q,1}_m K^1_m(q,m) + A^{n_q,2}_m K^2_m(q,m)\right) - \sum_{p=1}^{P} I_p K_1(q,p) = K_0(q). \tag{20}$$

The complete system of equations, considering the PEC elements, now has a size $(2M+1)(2N+1)+P$. A general view of the matrix form is given here for the sake of clarity:

$$\begin{bmatrix} S & -b_{PEC} \\ -K^1_m - K^2_m & -K_1 \end{bmatrix} \begin{bmatrix} x \\ I_{PEC} \end{bmatrix} = \begin{bmatrix} b_{source} \\ K_0 \end{bmatrix}, \tag{21}$$

where I_{PEC} is a vector of length P containing the unknowns I_p and b_{PEC} a matrix of size $(2M+1)(2N+1) \times P$ containing the PEC incident field contributions.

An illustrative case is shown in Fig. 3. Three PEC elements of radius $a_p = 150$µm, represented as red circles, are added compared to the structure of Fig. 2. The PEC elements are located $\lambda_g/4$ at the back of the source along the X-axis, in order to form a reflective backwall. They are distributed $\lambda_g/4$ apart from each other along the Y-axis. The presence of the backwall enhances the intensity of the electric field along the focusing direction of the lens. This reduces the side lobes (from -10dB to -13dB) and greatly reduces the backward radiation, as can be seen in red in Fig. 5.

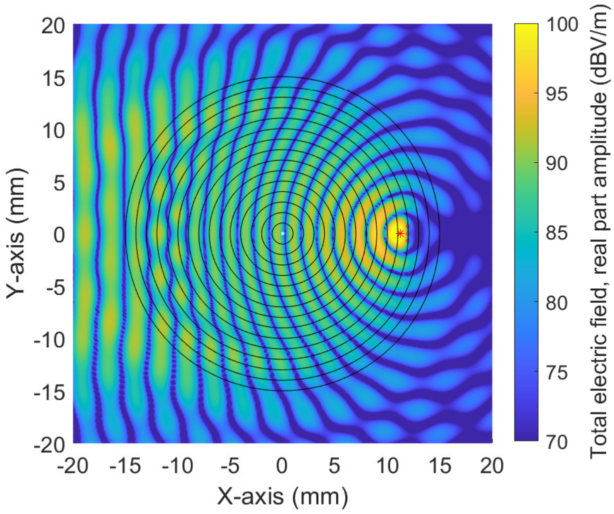

Fig. 3. Source located at the focal point $\rho' = f = 0.75\ a$ of a Gutman lens, with 3 PEC elements used as a backwall for the source.

In order to validate our 2D solver, we compared it with a 3D commercial simulator while assuming infinite thickness with uniform properties along the $\hat{z}$ axis. The structure presented in Fig. 3 was simulated in CST Microwave Studio. A discrete port acting as a current source was used as an excitation. A $z = 0$ cut of the total electric field is shown in Fig. 4 with the same range between 70dBV/m and 100dBV/m as in Fig. 3. The comparison with Fig. 3 clearly confirms the ability of our solver to cope with both a GRIN medium and the presence of PEC elements.

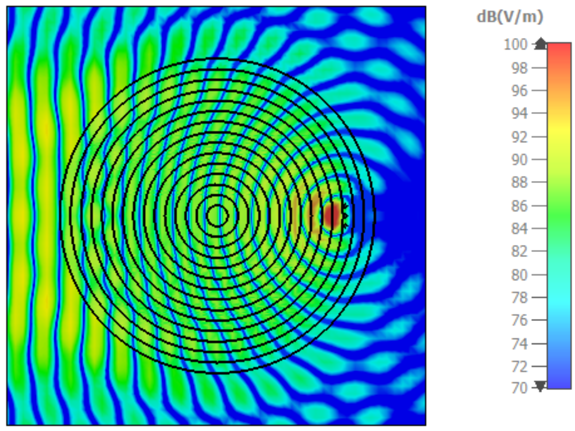

Fig. 4. CST Results for a source located at the focal point $\rho' = f = 0.75\ a$ of a Gutman lens, with 3 PEC elements used as a backwall for the source.

A last illustrative case is shown in Fig. 6. PEC elements of radius $a_p = 150$µm are added, compared to the structure of Fig. 2, at $\rho_p = 0.2\ a$ every 15°. The combination of electrically small PEC elements creates an equivalent electrically large

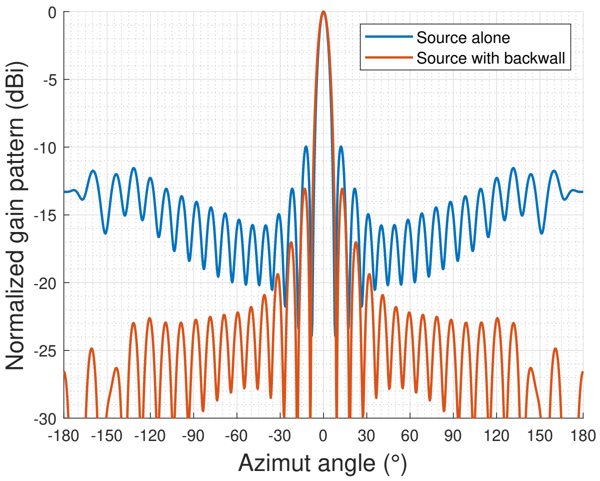

Fig. 5. Normalized radiation patterns corresponding to Fig. 2 and 3.

PEC cylinder, where there is no electric field. This can be an alternative approach to solve problems containing a PEC core layer such as [4] or [7], while avoiding the use of specific Green's functions for grounded cylindrically layered media.

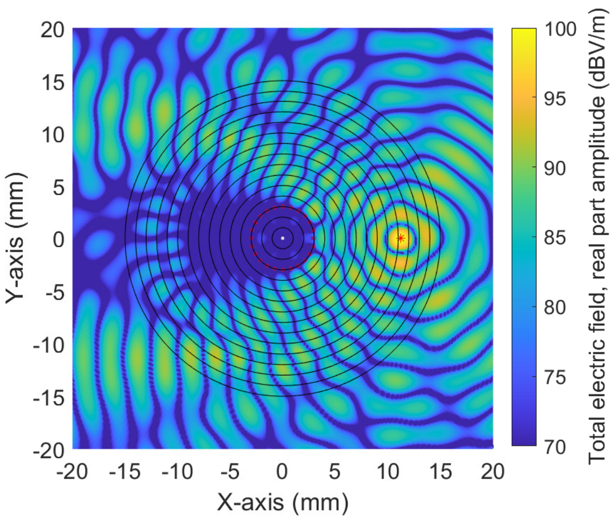

Fig. 6. Source located at the focal point $\rho' = f = 0.75\ a$ of a Gutman lens, with PEC elements arranged at $\rho_p = 0.2\ a$ every $15°$.

V. Conclusion

We established equations to solve the 2D problem of electromagnetic propagation by a source placed inside a GRIN lens, the latter possibly featuring cylindrical and electrically small PEC elements. We showed that PEC elements can enhance the radiation properties of such a lens. We believe that such a solver might be used to further improve GRIN lenses, for example by placing PEC elements in such a way to reduce side lobes or control coupling between multiple sources.

Acknowledgment

This work was conducted thanks to the collaboration between the ICTEAM Research Group and BEA Sensors Europe, and was funded by the Région Wallonne under the ”Doctorat en entreprise” framework of the SPW EER.

References

[1] W. C. Chew, *Waves and Fields in Inhomogeneous Media*. New York:IEEE Press, 1995.
[2] A. Fort, F. Keshmiri, G. R. Crusats, C. Craeye, and C. Oestges, “A body area propagation model derived from fundamental principles: Analytical analysis and comparison with measurements,” IEEE Trans. Antennas Propag., vol. 58, no. 2, pp. 503–514, Feb. 2010.
[3] A.Ye. Svezhentsev, V. Volski, S. Yan, and G.A.E. Vandenbosh, “Shaped Nanoantennas on Cylindrical and Planar Substrate,” in Proc. of the 2017 IEEE First Ukraine Conference on Electrical and Computer Engineering (UKRCON), May 29, 2017-June 2, 2017, Kiev, Ukraine, pp.650 – 654.
[4] J. Sun, C. F. Wang, L. W. Li, and M. S. Leong, “Further improvement for fast computation of mixed potential Green’s functions for cylindrically stratified media,” IEEE Trans. Antennas Propag., vol. 52, no. 11, pp.3026-3036, Nov. 2004.
[5] K. Naishadham and L. B. Felsen, “Dispersion of Waves Guided Along a Cylindrically Stratified Medium,” IEEE Trans. Antennas and Propag., vol. 41, no. 3, pp. 304-313, Mar. 1993.
[6] V. Erturk and R. G. Rojas, “Efficient computation of surface fields excited on a dielectric-coated circular cylinder,” IEEE Trans. Antennas Propag., vol. 48, no. 10, pp. 1507–1516, Oct. 2000.
[7] S. Karan, V. B. Erturk, and A. Altintas, “Closed-form Green’s function representations in cylindrically stratified media for method of moments applications,” IEEE Trans. Antennas Propag., vol. 57, no. 4, pp. 1158–1168, Apr. 2009.
[8] S. Raffaelli, Z. Sipus and P. -. Kildal, “Analysis and measurements of conformal patch array antennas on multilayer circular cylinder,” IEEE Trans. Antennas Propag., vol. 53, no. 3, pp. 1105-1113, Mar. 2005.
[9] A. Y. Svezhentsev, V. Volski, and G. A. E. Vandenbosch, “Plane wave scattering by cylindrically conformal periodic finite array with PEC and graphene patches,” in Proc. IEEE Ukrainian Microw. Week (UkrMW), Sep. 2020, pp. 692–695.
[10] A. Y. Svezhentsev, S. V. Dukhopelnykov, V. Volski, G. A. E. Vandenbosch and A. I. Nosich, “Microsized Graphene Helmholtz Resonator on Circular Dielectric Rod: A Tunable Sub-THz Frequency-Selective Scatterer,” IEEE Trans. Antennas Propag., vol. 70, no. 3, pp.2105-2113, Mar. 2022.
[11] K. Lock and P. Smith, “Plane wave scattering by a braided cylindrical shield using Method of Regularization,” 2013 International Symposium on Electromagnetic Theory, Hiroshima, Japan, 2013, pp. 1129-1132.